



UNIVERSITY OF LEEDS

This is a repository copy of *Optimization of Recombinant Membrane Protein Production in the Engineered Escherichia coli Strains SuptoxD and SuptoxR.*

White Rose Research Online URL for this paper:  
<http://eprints.whiterose.ac.uk/148537/>

Version: Accepted Version

---

**Article:**

Michou, M, Kapsalis, C, Pliotas, C [orcid.org/0000-0002-4309-4858](https://orcid.org/0000-0002-4309-4858) et al. (1 more author) (2019) Optimization of Recombinant Membrane Protein Production in the Engineered Escherichia coli Strains SuptoxD and SuptoxR. ACS Synthetic Biology, 8 (7). pp. 1631-1641. ISSN 2161-5063

<https://doi.org/10.1021/acssynbio.9b00120>

---

© 2019 American Chemical Society. This is an author produced version of a paper published in ACS synthetic biology. Uploaded in accordance with the publisher's self-archiving policy.

**Reuse**

Items deposited in White Rose Research Online are protected by copyright, with all rights reserved unless indicated otherwise. They may be downloaded and/or printed for private study, or other acts as permitted by national copyright laws. The publisher or other rights holders may allow further reproduction and re-use of the full text version. This is indicated by the licence information on the White Rose Research Online record for the item.

**Takedown**

If you consider content in White Rose Research Online to be in breach of UK law, please notify us by emailing [eprints@whiterose.ac.uk](mailto:eprints@whiterose.ac.uk) including the URL of the record and the reason for the withdrawal request.



[eprints@whiterose.ac.uk](mailto:eprints@whiterose.ac.uk)  
<https://eprints.whiterose.ac.uk/>

1 **Optimization of recombinant membrane protein production**  
2 **in the engineered Escherichia coli strains**  
3 **SuptoxD and SuptoxR**

4  
5 Myrsini Michou<sup>1,2</sup>, Charalampos Kapsalis<sup>3</sup>, Christos Pliotas<sup>3,4</sup> and Georgios Skretas<sup>1\*</sup>

6  
7 <sup>1</sup>Institute of Biology, Medicinal Chemistry & Biotechnology, National Hellenic  
8 Research Foundation, Athens, 11635, Greece

9 <sup>2</sup>Department of Biochemistry and Biotechnology, University of Thessaly, Larisa,  
10 41500, Greece

11 <sup>3</sup>Biomedical Sciences Research Complex, School of Biology, University of St  
12 Andrews, KY169ST, United Kingdom

13 <sup>4</sup>The Astbury Centre for Structural Molecular Biology, School of Biomedical  
14 Sciences, University of Leeds, LS2 9JT, United Kingdom

15

16 \*Corresponding author

17 Georgios Skretas  
18 Institute of Biology, Medicinal Chemistry & Biotechnology  
19 National Hellenic Research Foundation  
20 48 Vassileos Constantinou Ave  
21 11635 Athens  
22 Greece  
23 Tel: +302107273736  
24 Email: gskretas@eie.gr

25

26 **Abstract**

27 Membrane proteins execute a wide variety of critical biological functions in all living  
28 organisms and constitute approximately half of current targets for drug discovery. As  
29 in the case of soluble proteins, the bacterium *Escherichia coli* has served as a very  
30 popular overexpression host for biochemical/structural studies of membrane proteins  
31 as well. Bacterial recombinant membrane proteins production, however, is typically  
32 hampered by poor cellular accumulation and severe toxicity for the host, which leads  
33 to low levels of final biomass and minute volumetric yields. In previous work, we  
34 generated the engineered *E. coli* strains SuptoxD and SuptoxR, which upon co-  
35 expression of the effector genes *djlA* or *rraA*, respectively, can suppress the cytotoxicity  
36 caused by membrane protein overexpression and produce enhanced membrane protein  
37 yields. Here, we systematically looked for gene overexpression and culturing  
38 conditions that maximize the accumulation of membrane-integrated and well-folded  
39 recombinant MPs in these strains. We have found that, under optimal conditions,  
40 SuptoxD and SuptoxR achieve greatly enhanced recombinant membrane protein  
41 production for a variety of membrane proteins, irrespective of their archaeal, eubacterial  
42 or eukaryotic origin. Furthermore, we demonstrate that the use of these engineered  
43 strains enables the production of well-folded recombinant MPs of high quality and at  
44 high yields, which are suitable for functional and structural studies. We anticipate that  
45 SuptoxD and SuptoxR will become broadly utilized expression hosts for recombinant  
46 membrane protein production in bacteria.

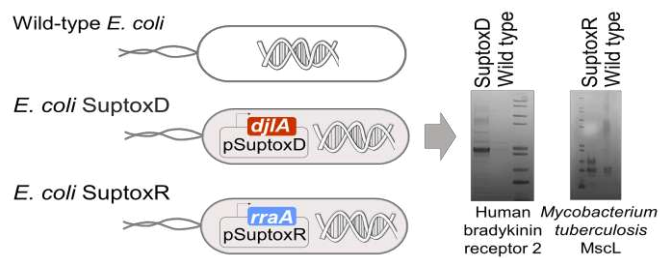
47

48

49

50 **For Table of Contents Use Only**

51



52

53 **Keywords**

54 Recombinant membrane protein production; toxicity; *E. coli* SuptoxD; *E. coli* SuptoxR;

55 *DjlA*; *RraA*

56

57 Membrane proteins (MPs) play key functional roles in all living organisms<sup>1</sup> and hold a  
58 prominent position among current targets for drug discovery<sup>2</sup>. As they are typically  
59 encountered in their native cells and tissues only at very small quantities, acquiring  
60 sufficient amounts of isolated MPs for biochemical and structural studies relies on their  
61 recombinant production in heterologous hosts, such as bacteria, yeasts, insect cells,  
62 mammalian cells and transgenic animals<sup>3</sup>.

63 As in the case of soluble proteins, the bacterium *Escherichia coli* has been one  
64 of the most popular overexpression hosts for production of recombinant MPs<sup>4,5</sup>. Among  
65 its many advantages, *E. coli* offer great simplicity, speed and low cost; relatively good  
66 understanding of the cell host's physiology; numerous tools for genetic manipulation<sup>5</sup>;  
67 high transformation efficiency coupled with established technologies for engineering  
68 the properties of the target MP<sup>6</sup>; and ability to be propagated in chemically defined  
69 medium allowing for substitution with selenomethionine for X-ray crystal structure  
70 determination<sup>7</sup> or with isotopically labeled amino acids for nuclear magnetic resonance  
71 structural studies<sup>8</sup>.

72 Bacterial MP production, however, is very often problematic, hampered by poor  
73 cellular accumulation and severe toxicity for the expression host<sup>4</sup>. MP-induced toxicity  
74 is a very frequent problem associated with recombinant MP production and it often  
75 leads to complete growth arrest, low levels of final biomass, and minute volumetric  
76 protein yields<sup>9-11</sup>. These unwanted phenomena occur most frequently for proteins of  
77 eukaryotic origin, which are also the ones of highest interest as targets for drug  
78 discovery.

79 In our previous work, we showed that we can engineer the bacterial protein  
80 synthesis machinery so as to generate modified *E. coli* strains with the ability to

81 withstand the toxicity caused by MP overexpression<sup>12</sup>. This allowed the development  
82 of specialized *E. coli* strains, which can be generally utilized for high-level recombinant  
83 MP production<sup>12</sup>. In order to achieve this, we sought single bacterial genes, whose co-  
84 expression can suppress MP overexpression-induced toxicity. After carrying out a  
85 genome-wide screen, we identified two highly potent suppressors: (i) *djlA*, the gene  
86 encoding for the membrane-bound DnaK co-chaperone DjlA<sup>13</sup>, and (ii) *rraA*, the gene  
87 encoding for RraA, an inhibitor of the mRNA-degrading activity of the *E. coli* RNase  
88 E<sup>14</sup>. *E. coli* strains co-expressing either *djlA* or *rraA*, which were named SuptoxD and  
89 SuptoxR, respectively, were found capable of accumulating significantly higher levels  
90 of final biomass and of producing dramatically enhanced yields for a variety of  
91 recombinant MPs in properly membrane-embedded form<sup>12, 15</sup>.

92         In the present work, we systematically looked for gene overexpression and  
93 culturing conditions that maximize the accumulation of membrane-integrated and well-  
94 folded recombinant MPs in *E. coli* SuptoxD and SuptoxR. We report that, under optimal  
95 conditions, SuptoxD and SuptoxR achieve greatly enhanced recombinant membrane  
96 protein production compared to wild-type *E. coli*, for a variety of both prokaryotic and  
97 eukaryotic MPs. Furthermore, we demonstrate that the use of these engineered strains  
98 enables the production of well-folded recombinant MPs at high quality and yields,  
99 which are suitable for functional and structural studies. Based on these results, we  
100 anticipate that SuptoxD and SuptoxR will become broadly utilized expression hosts for  
101 recombinant MP production in bacteria.

102

103

104

## 105 **Results and Discussion**

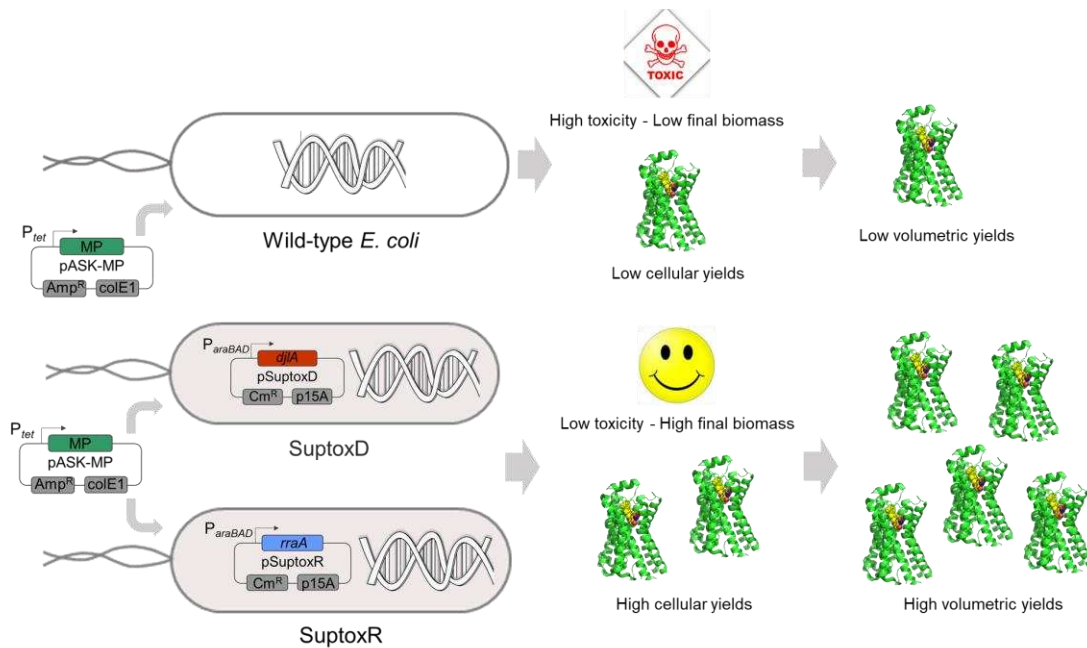
106 **Characteristics of the E. coli strains SuptoxD and SuptoxR.** E. coli SuptoxD and  
107 SuptoxR are two specialized strains for achieving high-level recombinant MP  
108 production in bacteria<sup>12</sup>. Their use has a dual positive effect on recombinant MP  
109 production: (i) it suppresses the toxicity that is frequently associated with MP  
110 overexpression, thus resulting in enhanced levels of final bacterial biomass, and (ii) it  
111 markedly enhances the cellular accumulation of membrane-incorporated and well-  
112 folded protein for a variety of recombinant MPs of both prokaryotic and eukaryotic  
113 origin<sup>12, 15</sup>. The combination of these two positive effects of MP production, results in  
114 greatly enhanced volumetric accumulation of recombinant MPs compared to wild-type  
115 E. coli <sup>12, 15</sup>.

116 The toxicity-suppressing and cellular production-promoting capabilities of  
117 SuptoxD and SuptoxR are based on the overexpression of either one of the effector  
118 genes *djlA* or *rraA*, respectively. In these strains, *djlA* and *rraA* are overexpressed from  
119 the vectors pSuptoxD and pSuptoxR, respectively, under the control of the *araBAD*  
120 promoter and its inducer L(+)-arabinose (Figure 1; Table 1)<sup>12</sup>. For the production of  
121 recombinant MPs in these strains, we typically use the vector pASK75<sup>16</sup> under the  
122 control of a tet promoter and its inducer anhydrotetracycline (aTc) (Figure 1; Table 1),  
123 although the enhanced MP productivity SuptoxD and SuptoxR is not promoter-  
124 dependent<sup>12, 15</sup>.

125

126

127



128

129 **Figure 1. Characteristics of the specialized MP-producing *E. coli* strains SuptoxD**  
 130 **and SuptoxR.** The toxicity-suppressing and cellular production-promoting capabilities  
 131 of SuptoxD and SuptoxR are based on the overexpression of either one of the effector  
 132 genes *djlA* or *rraA*, respectively. *djlA* and *rraA* are overexpressed from the vectors  
 133 pSuptoxD and pSuptoxR, respectively, under the control of the *araBAD* promoter and  
 134 its inducer L(+)-arabinose. For the production of recombinant MPs in these strains, we  
 135 typically use pASK75-based plasmids under the control of a tet promoter and its inducer  
 136 aTc (pASK-MP vector).

137

138 **Optimization of expression conditions for recombinant MP production in**  
 139 **SuptoxD and SuptoxR.** In order to determine optimal conditions for recombinant MP  
 140 production in SuptoxD and SuptoxR, we tested a range of different expression  
 141 parameters and looked for combinations that maximize volumetric accumulation of  
 142 membrane-integrated and folded MP. For fast expression monitoring, we utilized C-  
 143 terminal MP fusions with the green fluorescent protein (GFP) and recorded the levels  
 144 of cellular MP-GFP fluorescence corresponding to equal culture volumes (volumetric  
 145 accumulation) for each condition. This choice was based on the fact that the  
 146 fluorescence of *E. coli* cells expressing MP-GFP fusions has previously been found to

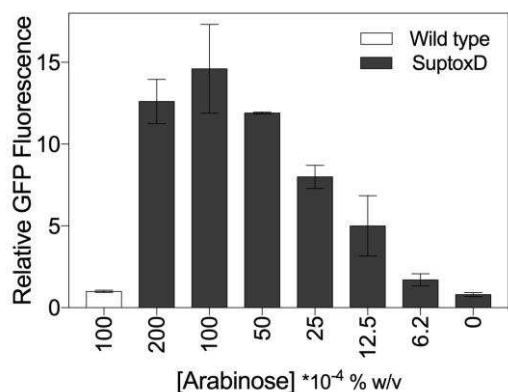
147 correlate well with the amount of membrane-integrated recombinant MP<sup>17</sup> and has been  
148 used extensively for facile monitoring of the accumulation levels of membrane-  
149 incorporated recombinant MPs, for optimization of overexpression parameters and for  
150 strain development, by us<sup>12, 15, 18-20</sup> and many others groups<sup>21-26</sup>.

151 We first evaluated the effect of varying the expression levels of the effector gene  
152 *djlA* in SuptoxD by changing the concentration of the inducer L(+)-arabinose in the  
153 growth medium. Arabinose concentrations in the range 0.0025-0.02% yielded maximal  
154 increases in volumetric cellular MP-GFP fluorescence compared to wild-type *E. coli*  
155 for two recombinant MPs tested: the human bradykinin receptor 2 (BR2) and the D03  
156 variant of the rat neurotensin receptor 1 (NTR1(D03))<sup>6</sup> (Table 1; Figures. 2a and b).  
157 Both MPs are members of the G protein-coupled receptor (GPCR) superfamily and are  
158 of high interest as targets for drug discovery<sup>27, 28</sup>. The three-dimensional structure of  
159 NTR1 has been solved recently<sup>27</sup>, while the structure of BR2 remains undetermined.  
160 Arabinose concentrations higher than 0.02% did not result in higher MP productivity,  
161 presumably due to the toxicity that is associated with strong *djlA* overexpression<sup>13, 29</sup>.  
162 Western blot and in-gel fluorescence analyses<sup>30</sup> of isolated total membrane fractions of  
163 wild type and SuptoxD cells producing NTR1(D03)-GFP verified that the enhanced  
164 MP-GFP fluorescence phenotypes observed occur due to increased production of full-  
165 length, membrane-embedded and well-folded recombinant MP (Figure 2c). Thus,  
166 addition of 0.0025-0.02% arabinose results in high-level production of recombinant  
167 MPs in *E. coli* SuptoxD, with an apparent optimum at 0.01%.

168 We next performed a similar analysis for the effector gene *rraA* in SuptoxR  
169 using again two model MPs: BR2 and the large conductance mechanosensitive ion  
170 channel (MscL) from *Mycobacterium tuberculosis* (Table 1). In this case, higher arabi-

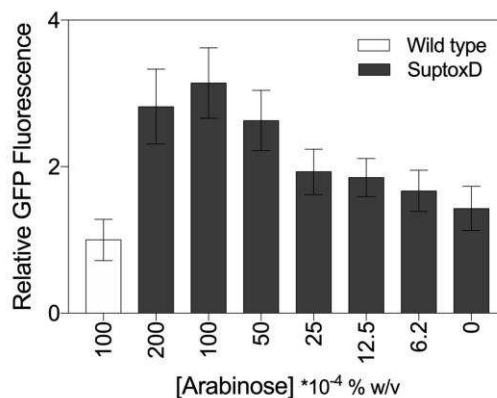
171

(a)



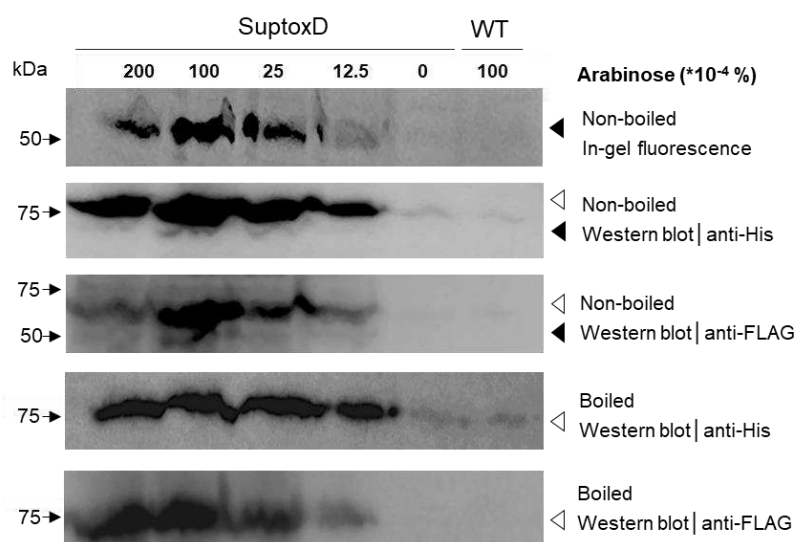
172

(b)



173

(c)

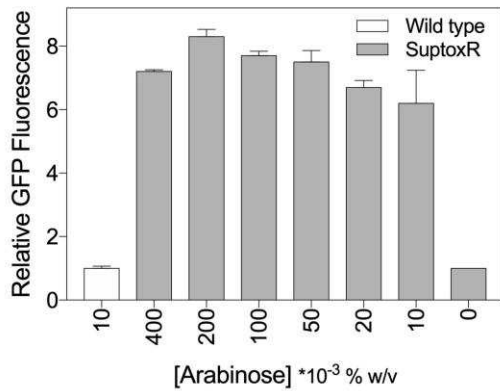


174

175 **Figure 2. Determination of the optimal levels of *djlA* co-expression for maximal**  
 176 **recombinant MP production in *E. coli* SuptoxD cells by arabinose titration. (a).**  
 177 Fluorescence of equal culture volumes of *E. coli* MC1061 (Wild type) and SuptoxD  
 178 cells producing BR2-GFP by the addition of 0.2  $\mu\text{g/ml}$  aTc and the indicated arabinose  
 179 concentrations for 16 h at 25 °C. The fluorescence of BR2-producing MC1061 cells  
 180 was arbitrarily set to one. (b). For NTR1(D03)-GFP as in (a). (c). Sodium dodecyl  
 181 sulfate polyacrylamide gel electrophoresis (SDS-PAGE)/western blot analysis of  
 182 isolated total membrane fractions of equal culture volumes of MC1061 (Wild type, WT)  
 183 and SuptoxD cells producing NTR1(D03)-GFP as described in (b), visualization of the  
 184 produced fusion by in-gel fluorescence and western blotting using a C-terminal anti-  
 185 polyhistidine or a N-terminal anti-FLAG antibody without (non-boiled) or with boiling  
 186 (boiled) of the samples prior to loading as indicated. The black and white arrows  
 187 indicate the positions of the fluorescent and non-fluorescent NTR1(D03)-GFP bands,  
 188 respectively. In (a) and (b), experiments were carried out in replica triplicates and the  
 189 error bars represent one standard deviation from the mean value.

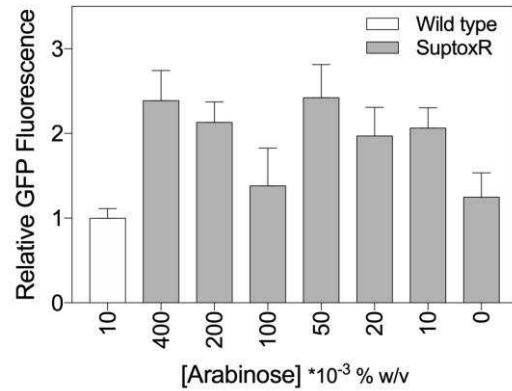
190

(a)



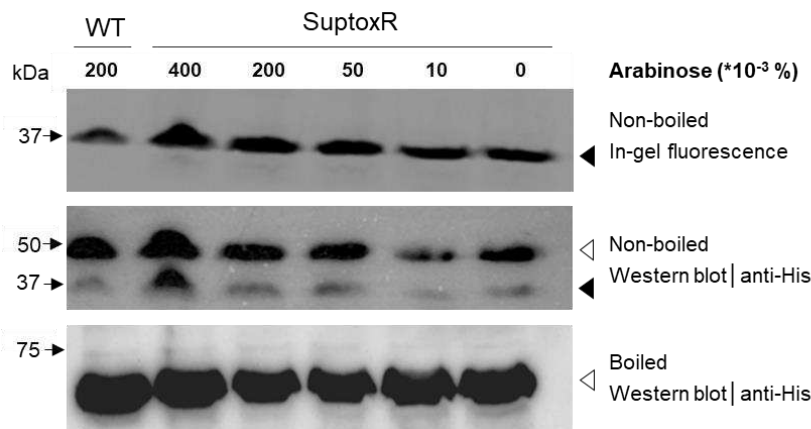
191

(b)



192

(c)



193

194 **Figure 3. Determination of the optimal levels of *rraA* co-expression for maximal**  
 195 **recombinant MP production in *E. coli* SuptoxR cells by arabinose titration. (a).**  
 196 Fluorescence of equal culture volumes of *E. coli* MC1061 (Wild type) and SuptoxR  
 197 cells producing BR2-GFP by the addition of 0.2  $\mu\text{g/ml}$  aTc and the indicated arabinose  
 198 concentrations for 16 h at 25 °C. The fluorescence of BR2-producing MC1061 cells  
 199 was arbitrarily set to one. Experiments were carried out in replica triplicates and the  
 200 error bars represent one standard deviation from the mean value. (b). For MscL-GFP  
 201 as in (a). Mean values  $\pm$  s.d. are presented ( $n=3$  independent experiments, each one  
 202 performed in replica triplicates). (c). SDS-PAGE/western blot analysis of isolated total  
 203 membrane fractions of equal culture volumes of MC1061 (Wild type, WT) and  
 204 SuptoxR cells producing MscL-GFP as described in (b), visualization of the produced  
 205 fusion by in-gel fluorescence and western blotting using a C-terminal anti-polyhistidine  
 206 antibody without (non-boiled) or with (boiled) boiling of the samples prior to loading  
 207 as indicated. The black and white arrows indicate the positions of the fluorescent and  
 208 non-fluorescent MscL-GFP bands, respectively.

209

210 nose concentrations in the range 0.01-0.4% were required for maximal recombinant MP  
211 production, with an apparent optimum at 0.2-0.4% (Figure 3).

212 Having established optimal cellular levels for DjlA and RraA, we searched for  
213 aTc concentrations that maximize overexpression of recombinant MPs in SuptoxD and  
214 SuptoxR. For both strains, 50-400 µg aTc per L of shake flask culture resulted in the  
215 highest accumulation of membrane-embedded, full-length and well-folded recombinant  
216 MP for all tested targets (Figures 4 and 5).

217 The incubation temperature, at which MP production occurs, had a strong  
218 impact on the final volumetric accumulation of recombinant MP for both SuptoxD and  
219 SuptoxR (Figure 6a). This is consistent with what has been observed previously with  
220 other strains and for other recombinant MPs<sup>22</sup>. Induction of protein production at 25 °C  
221 resulted in maximized productivity of recombinant MP for both SuptoxD and SuptoxR  
222 (Figure 6a).

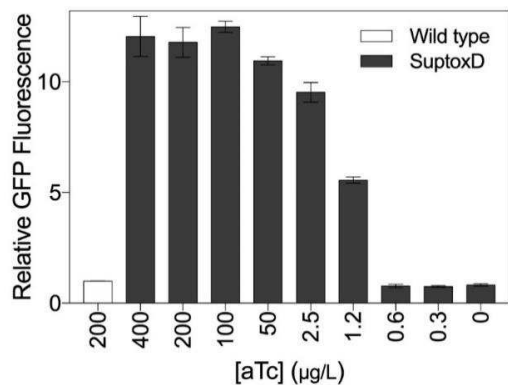
223 Under optimal production conditions (incubation temperature and inducer  
224 concentrations), the volumetric production of recombinant MP increased for both  
225 SuptoxD and SuptoxR until 12-14 h after aTc addition to the medium and leveled-off  
226 after that (Figure 6b). Importantly, even after 16 h continuous production of MPs,  
227 whose strong overexpression is severely toxic for *E. coli* and typically causes complete  
228 growth arrest following induction, such as BR2 and NTR1<sup>12, 20, 31</sup>, SuptoxD and  
229 SuptoxR cultures were homogeneous as revealed by flow cytometry analysis, thus  
230 demonstrating MP genetic stability in these strains (Figure 6c).

231

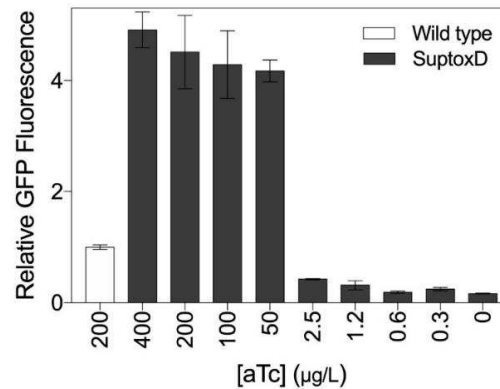
232

233

(a)



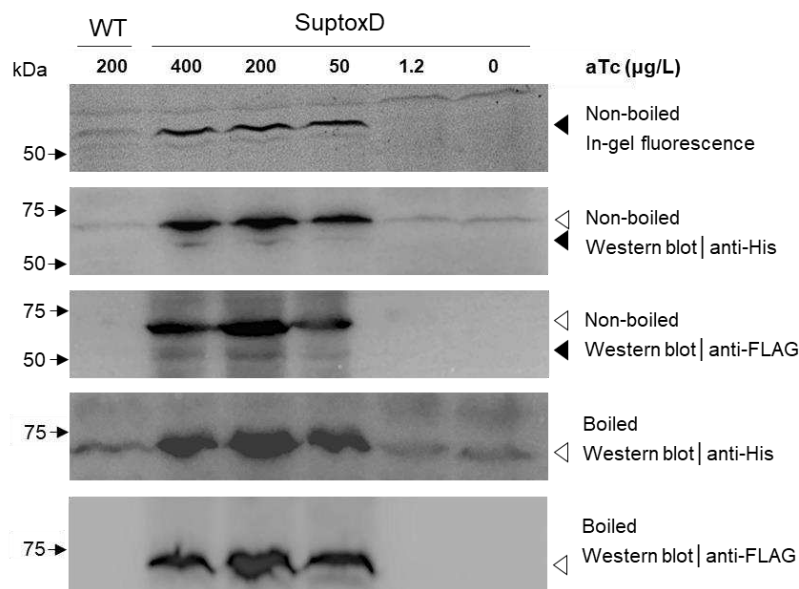
(b)



234

235

(c)

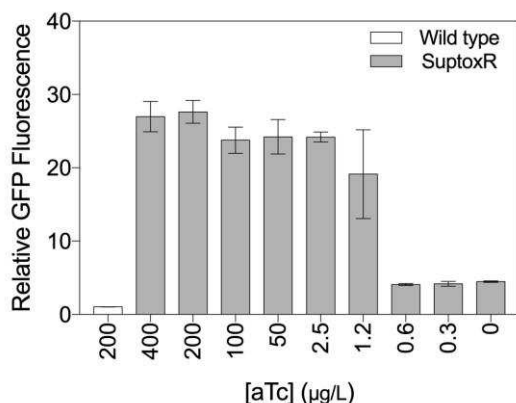


236

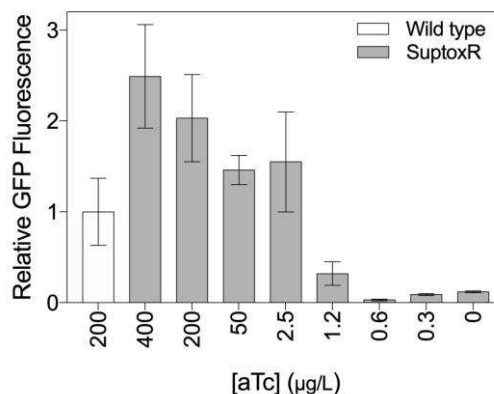
237 **Figure 4. Optimization of recombinant MP production in *E. coli* SuptoxD cells by**  
 238 **aTc titration. (a).** Fluorescence of equal culture volumes of *E. coli* MC1061 (Wild  
 239 type) and SuptoxD cells producing BR2-GFP by the addition of 0.01% arabinose for  
 240 16 h at 25 °C. The fluorescence of BR2-producing MC1061 cells was arbitrarily set to  
 241 one. (b). For NTR1(D03)-GFP as in (a). (c). SDS-PAGE/western blot analysis of  
 242 isolated total membrane fractions of equal culture volumes of MC1061 (Wild type, WT)  
 243 and SuptoxD cells producing NTR1(D03)-GFP as described in (b), visualization of the  
 244 produced fusion by in-gel fluorescence and western blotting using a C-terminal anti-  
 245 polyhistidine or a N-terminal anti-FLAG antibody without (non-boiled) or with boiling  
 246 (boiled) of the samples prior to loading as indicated. The black and white arrows  
 247 indicate the positions of the fluorescent and non-fluorescent NTR1(D03)-GFP bands,  
 248 respectively. In (a) and (b), experiments were carried out in replica triplicates and the  
 249 error bars represent one standard deviation from the mean value.

250

(a)

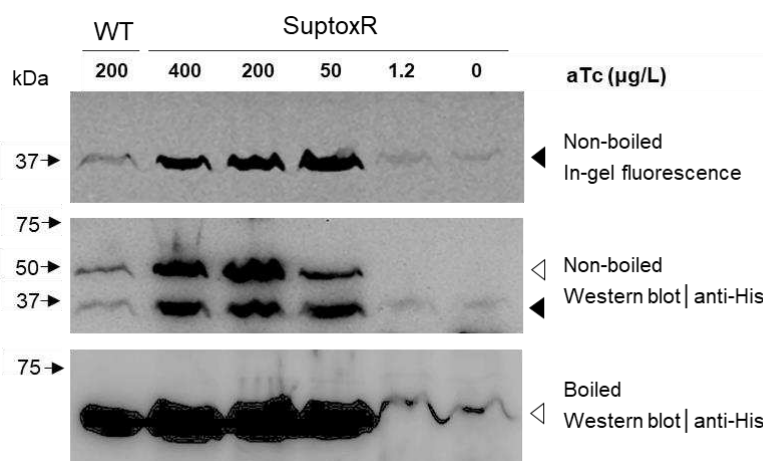


(b)



251

252 (c)



253

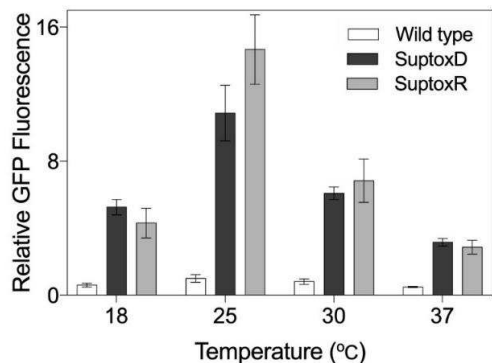
254

255 **Figure 5. Optimization of recombinant MP production in E.coli SuptoxR cells by**  
 256 **aTc titration. (a).** Fluorescence of equal culture volumes of E. coli MC1061 (Wild  
 257 type) and SuptoxR cells producing BR2-GFP by the addition of 0.2% arabinose for 16  
 258 h at 25 °C. The fluorescence of BR2-producing MC1061 cells was arbitrarily set to one.  
 259 **(b).** For MscL-GFP as in (a). **(c).** SDS-PAGE/western blot analysis of isolated total  
 260 membrane fractions of equal culture volumes of MC1061 (wild type, WT) and SuptoxR  
 261 cells producing MscL-GFP as described in (b), visualization of the produced fusion by  
 262 in-gel fluorescence and western blotting using a C-terminal anti-polyhistidine antibody  
 263 without (non-boiled) or with (boiled) boiling of the samples prior to loading as  
 264 indicated. The black and white arrows indicate the positions of the fluorescent and non-  
 265 fluorescent MscL-GFP bands, respectively. In (a) and (b), experiments were carried out  
 266 in replica triplicates and the error bars represent one standard deviation from the mean  
 267 value.

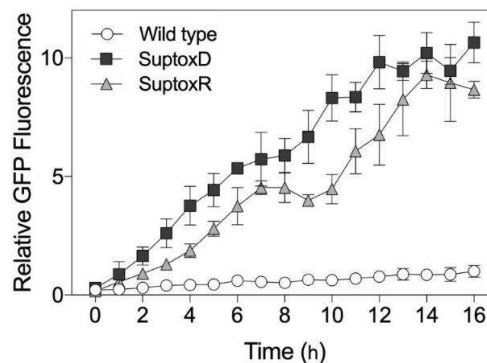
268

269

(a)



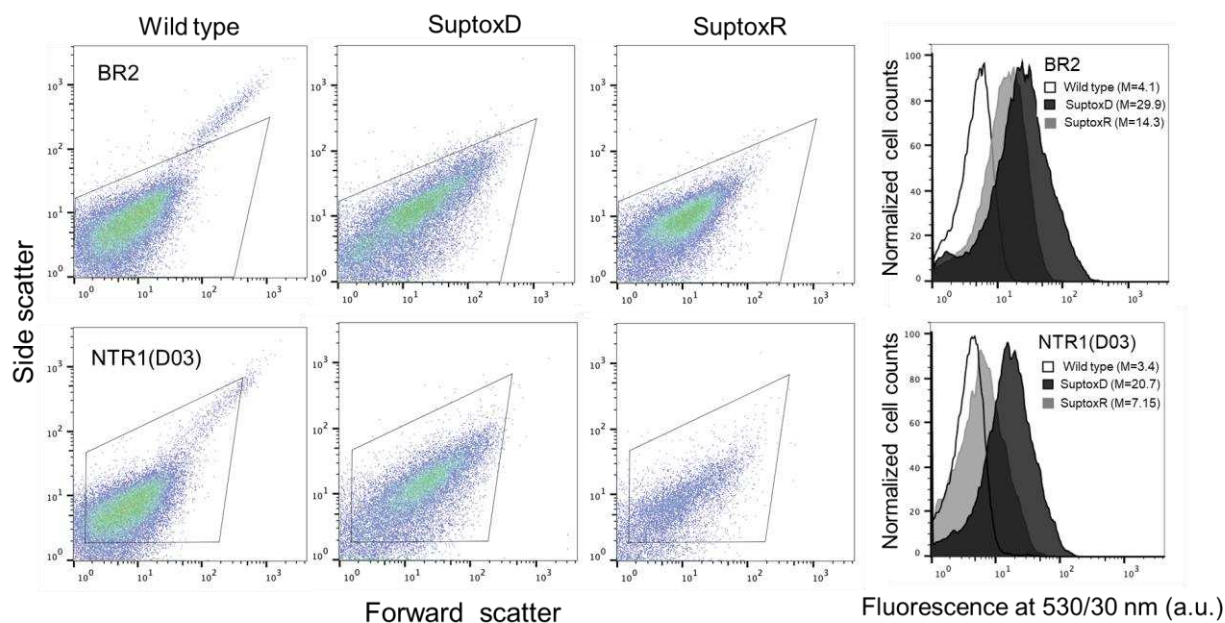
(b)



270

271

(c)



272

273 **Figure 6. Determination of optimal culturing temperature and time for**  
 274 **recombinant MP production in E. coli SuptoxD and SuptoxR.** (a). Fluorescence of  
 275 E. coli MC1061 (Wild type), SuptoxD and SuptoxR cells producing BR2-GFP by the  
 276 addition of 0.2  $\mu\text{g/ml}$  aTc and 0.01% (SuptoxD) or 0.2% (SuptoxR) arabinose at the  
 277 indicated temperatures overnight. Mean values  $\pm$  s.d. are presented (n=3 independent  
 278 experiments, each one performed in replica triplicates). The fluorescence of BR2-  
 279 producing MC1061 cells at 25  $^{\circ}\text{C}$  was arbitrarily set to one. (b). Comparison of the  
 280 fluorescence of equal culture volumes of E. coli MC1061 (wild type), SuptoxD and  
 281 SuptoxR cells producing BR2-GFP by the addition of 0.2  $\mu\text{g/mL}$  aTc and 0.01%  
 282 (SuptoxD) or 0.2% (SuptoxR) arabinose overnight at 25  $^{\circ}\text{C}$  at different time points after  
 283 aTc addition to the medium. The fluorescence of BR2-producing MC1061 cells at 16 h  
 284 was arbitrarily set to one. Experiments were carried out in replica triplicates and the  
 285 error bars represent one standard deviation from the mean value. (c). (Left) Forward  
 286 versus side scatter plots as determined by flow cytometry analysis of E. coli MC1061

287 (Wild type), SuptoxD and SuptoxR cells producing BR2-GFP or NTR1(D03)-GFP by  
288 the addition of 0.2 µg/mL aTc and 0.01% (SuptoxD) or 0.2% (SuptoxR) arabinose for  
289 16 h at 25 °C. (Right) Comparison of the levels of individual cell fluorescence of E.  
290 coli MC1061 (Wild type), SuptoxD and SuptoxR cells producing BR2-GFP or  
291 NTR1(D03)-GFP(bottom) as measured by flow cytometry. Cells were gated as  
292 indicated by the grey line (left). Fluorescence measurements correspond to the mean  
293 value (M) of replica experiments performed in triplicate.

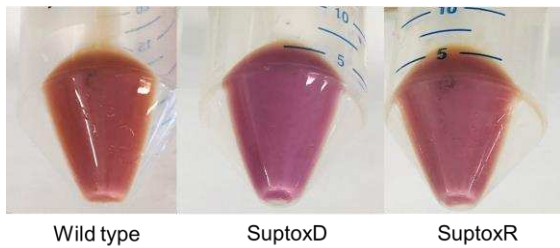
294

295 **SuptoxD and SuptoxR achieve enhanced production of detergent-extractable and**  
296 **functional recombinant MP.** Our results indicate that, under optimal conditions,  
297 SuptoxD and SuptoxR achieve greatly enhanced production of full-length, membrane-  
298 embedded and well-folded recombinant MPs compared to wild-type E. coli. In order to  
299 test whether these enhanced amounts contain biologically active protein and, thus,  
300 would be suitable for functional studies, we compared the accumulation of the archaeal  
301 deltarhodopsin from *Haloterrigena turkmenica* (HtdR) in wild-type E. coli and  
302 SuptoxD/SuptoxR. HtdR is a light-driven outwards proton pump, which when properly  
303 folded, can bind the chromophore all-trans-retinal and acquires a characteristic purple  
304 color with an adsorption maximum at ~550 nm<sup>32</sup>. Apart from model proteins for  
305 convenient monitoring of functional protein production<sup>33</sup>, microbial rhodopsins are also  
306 invaluable tools for optogenetic regulation applications<sup>30</sup>. E. coli has served as a cell  
307 factory for recombinant production of this type of MPs for biochemical and structural  
308 studies<sup>34, 35</sup>, as well as for the engineering of protein variants with new properties<sup>36, 37</sup>.  
309 Under optimal MP production conditions, our strains were found to accumulate  
310 significantly enhanced levels of both total and detergent-extractable functional HtdR  
311 (Figure 7).

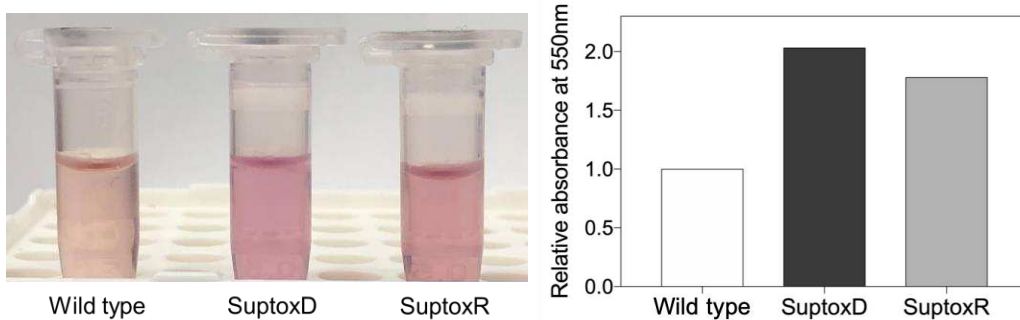
312

313

314 (a)



316 (b)

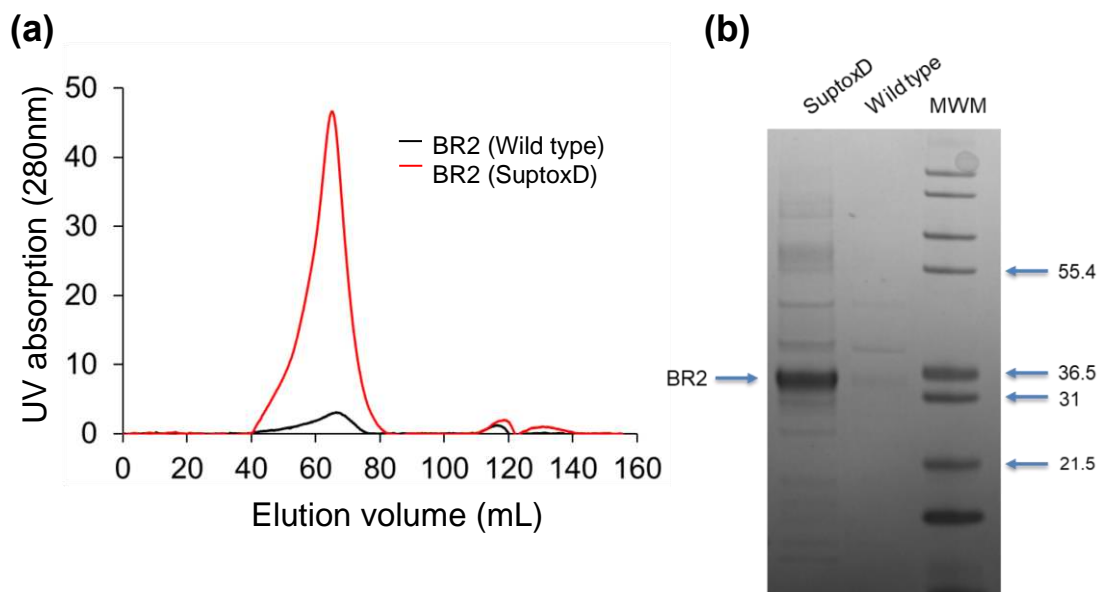


318 **Figure 7. SuptoxD and SuptoxR produce enhanced amounts of functional**  
319 **recombinant MP.** (a). Photographs of purple-colored pellets derived from equal  
320 culture volumes of MC1061 (Wild type), SuptoxD and SuptoxR cells producing HtdR  
321 by the addition of 0.2  $\mu\text{g}/\text{mL}$  aTc and 0.01% (SuptoxD) or 0.2% (SuptoxR) arabinose  
322 for 16 h at 25  $^{\circ}\text{C}$  in the presence of 10  $\mu\text{M}$  all-trans-retinal. (b). (Left) Photographs of  
323 DDM-extracted HtdR acquired from the total lysates of equal culture volumes of the  
324 MC1061 (Wild type), SuptoxD and SuptoxR cells shown in (a). (Right) Relative  
325 absorbance at 550 nm of the samples shown in (b), left.

326

327 **SuptoxD and SuptoxR achieve greatly enhanced production of purified**  
328 **recombinant MPs.** Structural and biophysical studies of MPs typically require the  
329 availability of mg quantities of detergent-extracted and isolated protein in a folded state.  
330 The required yields of purified protein from an MP-overexpression strain for such  
331 purposes should be in the range 0.2-1 mg per L of cell culture<sup>3</sup>. To determine the yields  
332 of purified recombinant MPs expressed in our strains, we produced polyhistidine-  
333 tagged versions of BR2 in SuptoxD and the MscL variant F88C (see below) in SuptoxR  
334 under the optimal expression conditions determined above. Both MPs were solubilized

335 from isolated total membranes in detergent and were purified using immobilized metal  
336 affinity chromatography (IMAC), followed by size-exclusion chromatography (SEC).  
337 BR2 was extracted using fos-choline-14 (Fos14), while MscL using n-dodecyl  $\beta$ -D-  
338 maltoside (DDM). For both MPs, we performed control purification experiments from  
339 wild-type *E. coli* under identical conditions. The yield of isolated BR2 from SuptoxD  
340 was found to be ~1 mg per L of shake flask culture. This is approximately 14-fold  
341 higher than the corresponding yield from wild-type *E. coli* (~47.4 mAU absorption for  
342 SuptoxD compared to ~3.5 mAU for wild type) (Figure 8a). BR2 isolated from  
343 SuptoxD eluted as a single peak in SEC, indicating that purified protein in DDM  
344 solution is folded and non-aggregated (Figure 8a).

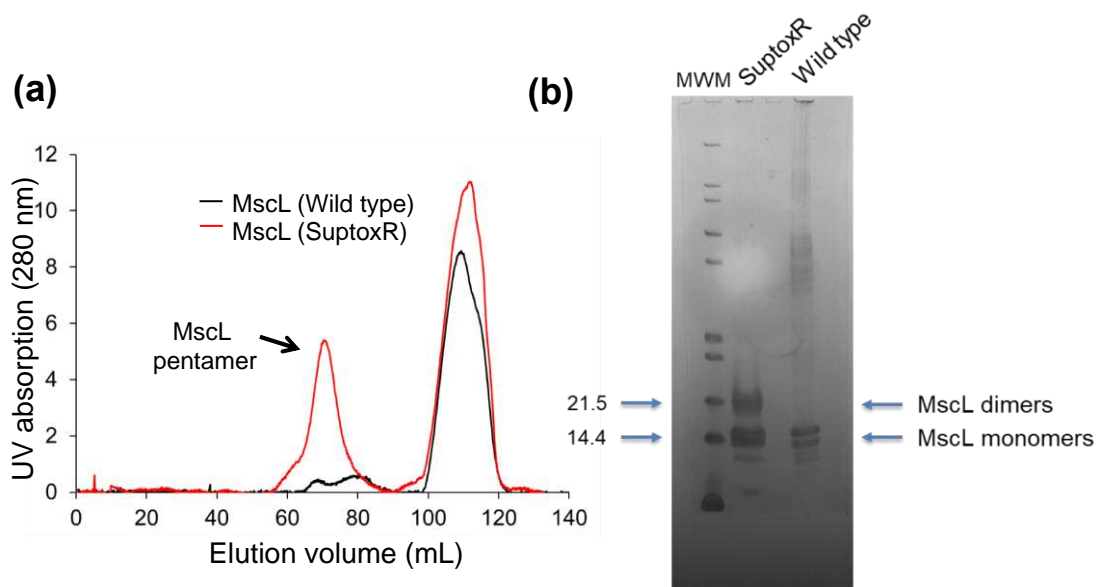


345

346 **Figure 8. *E. coli* SuptoxD produce greatly enhanced amounts of isolated**  
347 **recombinant MP. (a).** SEC profiles of purified BR2 from *E. coli* MC1061 (Wild type;  
348 black) and SuptoxD (red) **(b).** SDS-PAGE analysis of the BR2 SEC peaks (~67 mL on  
349 a Superdex200 16/60 GE column) obtained in (a). MWM: molecular weight marker.  
350 The numbers indicate the corresponding molecular masses in kDa.

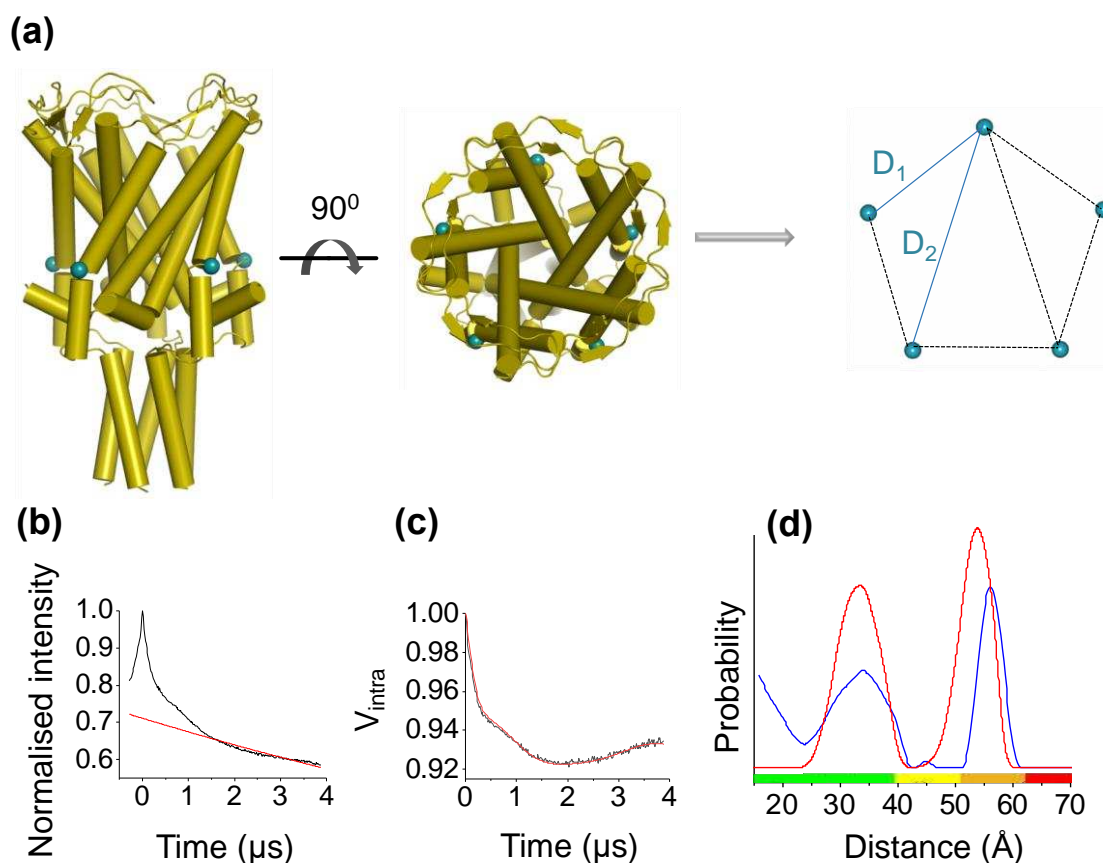
351

352 The purity of the SEC peaks of the isolated BR2 was assessed by SDS-PAGE analysis.  
 353 This revealed adequate sample purity for initial screening and characterization purposes  
 354 (Figure 8b). The strong single band appearing after BR2 purification from SuptoxD  
 355 exhibited the expected electrophoretic mobility corresponding to apparent molecular  
 356 mass of ~35 kDa (detergent-extracted BR2 and other MPs run faster on SDS-PAGE  
 357 than expected according to their molecular weight<sup>31, 38</sup>) and its identity was confirmed  
 358 by western blot analysis and mass spectrometry following trypsin digestion  
 359 (Supplementary Figure S1). It is important to note, that human BR2 is a particularly  
 360 challenging MP to produce recombinantly, not only in microbial expression hosts<sup>31</sup> but  
 361 also in human cell cultures<sup>38</sup>.



362

363 **Figure 9. E. coli SuptoxR produce greatly enhanced amounts of isolated**  
 364 **recombinant MP. (a).** SEC profiles of purified MscL from E. coli MC1061 (Wild type;  
 365 black) and SuptoxR (red), revealing a single homogeneous monodisperse peak of MscL  
 366 pentamers. **(b).** SDS-PAGE analysis of the pentameric MscL(F88C) SEC peaks  
 367 obtained from (a). The gel indicates the presence of highly pure protein containing only  
 368 MscL(F88C) monomers and disulfide-linked dimers. F88C is located at the interface of  
 369 two neighboring subunits and the appearance of reducing agent-resistant disulfide-  
 370 linked dimers is in agreement with previous studies of single cysteine mutants of both  
 371 E. coli MscL and the small conductance mechanosensitive ion channel (MscS)<sup>39, 40</sup>.  
 372 MWM: molecular weight marker. The numbers indicate the corresponding molecular  
 373 masses in kDa.



374

375 **Figure 10. E. coli SuptoxR produce well-folded MP at the expected**  
 376 **oligomerization and conformational state. (a).** Side and top MscL channel pore view.  
 377 F88C is highlighted (cyan spheres). Pentameric MscL is labelled with five spin labels  
 378 resulting in pentagon symmetry and thus two expected distances in PELDOR/DEER.  
 379 **(b).** Raw, uncorrected time domain spectrum (black) with the background function  
 380 (red). **(c).** Background corrected time domain spectrum (black) with the fitting function  
 381 (red). **(d).** PELDOR distance distribution of MscL(F88C) covalently modified with  
 382 MTSSL (blue area, corresponding to mean  $\pm 2\sigma$  confidence interval as calculated by the  
 383 DeerAnalysis validation tool) compared to in silico-modelled distances (red) of the  
 384 MscL crystal structure (PDB 2OAR), using MtsslWizard. The rainbow colour bar  
 385 indicates the reliability of the distance range (calculated by DeerAnalysis), based on the  
 386 experimental 4  $\mu$ s time window used.

387

388 Similarly to the results acquired with SuptoxD, a >10-fold increased yield was  
 389 observed for the purified mechanosensitive ion channel MscL in SuptoxR compared to  
 390 wild-type E. coli (~5.40 mAU absorption for SuptoxD compared to ~0.47 for wild-  
 391 type) (Figure 9a). The yields of purified MscL were calculated to be ~0.33 mg and 0.03

392 mg per L of shake flask culture for SuptoxR and wild-type *E. coli*, respectively. The  
393 recorded SEC peak for SuptoxR-purified MscL was monodisperse and highly  
394 homogeneous and eluted at ~69 mL from a Superdex200 16/60 column, thus indicating  
395 a highly monodisperse and well-folded multimeric channel protein. The purity of these  
396 SEC peaks was further assessed by SDS-PAGE (Figure 9b) and the identity of the MscL  
397 bands was confirmed by mass spectrometry (Supplementary Figure S2).

398 In order to assess whether the SuptoxR-produced MscL is well folded and so as  
399 to determine its oligomeric and conformational state in DDM solution, we combined  
400 pulsed electron double resonance (PELDOR) (also known as double electron  
401 electron resonance (DEER)) spectroscopy with site-directed spin labelling<sup>41-43</sup>. This  
402 method allows for measurement of interspin distances of engineered/introduced  
403 paramagnetic species (carrying unpaired electrons) within protein complexes between  
404 1.5 to 7 nm and irrespective of their size. PELDOR has served as a powerful tool for  
405 studying conformation, oligomeric state and complex dynamics of various MP types,  
406 such as ion channels, transporters and GPCRs<sup>39, 44-49</sup>, at molecular resolution and in  
407 complete agreement with X-ray crystallography studies<sup>50</sup>. To perform PELDOR  
408 analysis of MscL, we introduced the S-(2,2,5,5-tetramethyl-2,5-dihydro-1H-pyrrol-3-  
409 yl)methyl methanesulfonylthioate (MTSSL) spin label by covalent attachment to the  
410 single-cysteine variant MscL (F88C), resulting in a MscL pentamer carrying five spins  
411 per macromolecule (Figure 10a). Due to the expected pentagon symmetry, two distinct  
412 distances, i.e.  $D_1$  and  $D_2$ , are anticipated (Figure 10a), thus allowing the determination  
413 of the oligomerization and conformational state of the purified MscL in detergent  
414 solution. We obtained a PELDOR time trace with clear dipolar oscillations in the raw  
415 data and a 4- $\mu$ s time window (Figure 10b), which allowed accurate distances to be  
416 determined, after background correction (Figures 10c and d). The resulting distance

417 distribution was in very good agreement with the in silico modelled distances of the  
418 closed state pentameric MscL (PDB 2OAR)<sup>51</sup>, suggesting that the SuptoxR-produced  
419 MscL channel is correctly folded and adopts a symmetric pentameric arrangement in  
420 the closed conformation. The pentameric state of the SuptoxR-isolated MscL was  
421 further confirmed by the resulting distance peak ratio  $D_2/D_1 \sim 1.6$  (for a perfectly  
422 symmetric pentamer this ratio is 1.6<sup>41</sup>). PELDOR/DEER, therefore, provides robust  
423 experimental evidence for the correct folding and structural integrity of the MscL  
424 channel protein produced in SuptoxR.

425 Overall, our results demonstrate that *E. coli* SuptoxD and SuptoxR are two  
426 specialized strains that achieve greatly enhanced recombinant MP production in  
427 bacteria. In our present and previous work<sup>12, 15</sup> we have found that this enhanced  
428 productivity occurs for membrane proteins (1) from all three domains of life (archaeal,  
429 eubacterial and eukaryotic); (2) with different functions (GPCR, mechanosensitive  
430 channel, light-driven proton pump proton pump and other); and (3) with different  
431 molecular and topological characteristics (size, number of transmembrane helices,  
432 oligomerization states etc.). Under the optimized production conditions determined  
433 here, the use of these strains allows the production of high-quality recombinant MPs at  
434 quantities sufficient for functional and structural studies. Recombinant MP production  
435 in these strains yields well-folded and homogeneous proteins, which maintain their  
436 structural integrity. Based on these results, we anticipate that SuptoxD and SuptoxR  
437 will become broadly utilized expression hosts for recombinant MP production in  
438 bacteria.

439

440



464 **MP overexpression in liquid cultures.** *E. coli* cells freshly transformed with the  
465 appropriate expression vector(s) were used for all protein production experiments.  
466 Single bacterial colonies were used to inoculate liquid LB cultures containing the  
467 appropriate combination of antibiotics (100 µg/mL ampicillin, 40 µg/mL  
468 chloramphenicol or 50 µg/mL kanamycin (Sigma)). These cultures were used with a  
469 1:50 dilution to inoculate fresh LB cultures with 0.01% (MC1061 and SuptoxD) or  
470 0.2% arabinose (SuptoxR), which were grown at 30 °C to an optical density at 600 nm  
471 (OD<sub>600</sub>) of ~0.3–0.5 with shaking, unless specified otherwise. The temperature was  
472 then decreased to 25 °C and after a temperature equilibration period of 10–20 min, MP  
473 expression was induced by the addition of 0.2 µg/mL aTc (Sigma) overnight, unless  
474 specified otherwise. For rhodopsin overproduction, we followed the same procedure,  
475 but when the cell density reached OD<sub>600</sub> ~0.3–0.5, protein production was induced by  
476 the addition of 0.2 µg/mL aTc in the presence of 10 µM all-trans-retinal (Cayman  
477 Chemical) overnight in dark.

478 **Membrane isolation.** Total membrane fractions were isolated from 1 L LB cultures in  
479 all cases, except for rhodopsin (250 mL). Cells were harvested by centrifugation (4,000  
480 x g for 10 min) and resuspended in 10 mL of cold lysis buffer (300 mM NaCl, 50 mM  
481 NaH<sub>2</sub>PO<sub>4</sub>, 15% glycerol, 5 mM dithiothreitol, pH 7.5). The cells were lysed by brief  
482 sonication steps on ice and the resulting lysates were clarified by centrifugation at  
483 10,000 x g for 15 min. The supernatant was then subjected to ultracentrifugation on a  
484 Beckman 70Ti rotor at 42,000 rpm (130,000 x g) for 1 h at 4 °C. The resulting pellet  
485 was finally re-suspended in 5 mL of cold lysis buffer and homogenized.

486 **Western blot and in-gel fluorescence analyses.** Proteins samples were analyzed by  
487 sodium dodecyl sulfate–polyacrylamide gel electrophoresis (SDS–PAGE) in 12-15%

488 gels with or without prior boiling of the samples for 10 min for western blotting and  
489 without prior boiling for in-gel fluorescence analysis. In-gel fluorescence was analyzed  
490 on a UVP ChemiDoc-It<sup>2</sup> Imaging System equipped with a CCD camera and a GFP  
491 filter, after exposure for about 3 s. For western blotting, proteins were transferred to  
492 polyvinylidene fluoride (PVDF) membranes (Merck) for 45 min at 12 V on a semidry  
493 blotter (Thermo Scientific). Membranes were blocked with 5% nonfat dried milk in  
494 Tris- buffered saline containing 0.1% Tween-20 (TBST) for 1 h at room temperature.  
495 After washing with TBST three times, membranes were incubated with the appropriate  
496 antibody dilution in TBST containing 0.5% nonfat dried milk at room temperature for  
497 1 h. The utilized antibodies were a mouse monoclonal antipolyhistidine antibody  
498 (Sigma) at 1:3,000 dilution (conjugated with horseradish peroxidase), a mouse  
499 monoclonal anti-FLAG antibody (Sigma) at 1:1,000 dilution, with a horseradish  
500 peroxidase-conjugated goat anti-mouse as secondary antibody at 1:5,000 dilution. The  
501 proteins were visualized using a ChemiDoc-It<sup>2</sup> Imaging System (UVP).

502 **Bulk fluorescence measurements.** Cells corresponding to 0.5 mL of culture were  
503 harvested and resuspended in 100  $\mu$ L PBS. The cell suspension was then transferred to  
504 a black 96-well plate and after fluorophore excitation at 488 nm, fluorescence was  
505 measured at 510 nm using a TECAN SAFIRE plate reader.

506 **Fluorescence analysis by flow cytometry.**  $\sim 10^7$  cells were re-suspended in 1 mL PBS  
507 and after fluorophore excitation at 488 nm, the fluorescence of 50,000 cells was  
508 measured at 530/30 nm using a CyFlow ML flow cytometer (Partec) and analyzed  
509 statistically using FlowJo 7.6.2.

510 **Rhodopsin extraction and quantification.** Pellets from 250 mL of cell culture were  
511 re-suspended in 7.5 ml cold lysis buffer. Cells were lysed by brief sonication steps on

512 ice and rhodopsin was extracted from total cell lysates by the addition of 2.5% (w/v)  
513 DDM (Glycon Biochemicals) and rotation at 180 rpm for 24 h at 4 °C in the dark. The  
514 mixture was subjected to ultra-centrifugation and, if a colorless pellet was acquired,  
515 the supernatant (detergent-extractable fraction) was collected analyzed by measuring  
516 absorbance at 550 nm as described previously<sup>32, 52</sup>.

517 **MscL and BR2 purification.** MscL(F88C) was expressed in E. coli MC161 (wild type)  
518 and SuptoxR, spin labelled and purified as previously described<sup>41, 48</sup>. The extent of  
519 cysteine modification (i.e. spin labelling efficiency) was assessed as previously  
520 described<sup>53</sup>. In brief, protein pellets were resuspended in phosphate-buffered saline  
521 (PBS), lysed with a cell disrupter at 30,000 psi and centrifuged at 4,000 x g for 20 min.  
522 The supernatant was then ultra-centrifuged at 100,000 x g for 1 h. The resulting  
523 membrane pellet was mechanically resuspended in solubilisation buffer (50 mM  
524 sodium phosphate of pH 7.5, 300 mM NaCl, 10% v/v glycerol, 50 mM imidazole, 1.5%  
525 w/v DDM (Glycon, GmbH) and incubated at 4 °C for 1 h. The sample was then  
526 centrifuged at 4,000 x g for 10 min and the supernatant was passed through a column  
527 containing 0.5 mL Ni<sup>2+</sup>-nitrilotriacetic acid (Ni<sup>2+</sup>-NTA) beads (Sigma). Subsequently,  
528 the column was washed with 10 mL wash buffer (50 mM sodium phosphate pH 7.5,  
529 300 mM NaCl, 10% v/v glycerol, 50 mM imidazole, 0.05% w/v DDM) and 5 mL wash  
530 buffer supplemented with 3 mM tris(2-carboxyethyl)phosphine (TCEP). Then, MTSSL  
531 (Glycon) dissolved in wash buffer at 10x excess of the expected protein concentration  
532 was added to the column and left to react for 2 h at 4 °C. The protein was then eluted  
533 with 5 mL of elution buffer (50 mM sodium phosphate of pH 7.5, 300 mM NaCl, 10%  
534 v/v glycerol, 300 mM imidazole, 0.05% w/v DDM) before being subjected to SEC  
535 using a Superdex 200 column (GE Healthcare) equilibrated with SEC buffer (50 mM

536 sodium phosphate of pH 7.5, 300 mM NaCl, 0.05% w/v DDM). Finally, the protein  
537 was concentrated to ~800  $\mu$ M monomer concentration for PELDOR measurements.

538 The purification protocol used for BR2 from *E. coli* MC161 (wild type) and  
539 SuptoxD was similar, with the exception that different buffers were used: solubilisation  
540 buffer (10 mM HEPES of pH 7.2, 400 mM NaCl, 10% v/v glycerol, 30 mM imidazole,  
541 0.5% w/v fos-14 (Anatrace) wash buffer (10 mM HEPES of pH 7.2, 400 mM NaCl,  
542 10% v/v glycerol, 30 mM imidazole, 0.05% w/v DDM); elution buffer (10 mM HEPES  
543 of pH 7.2, 400 mM NaCl, 10% v/v glycerol, 300 mM imidazole, 0.05% w/v DDM);  
544 and SEC buffer (10 mM HEPES of pH 7.2, 400 mM NaCl, 0.05% w/v DDM).

545 **PELDOR measurements, data analysis and in silico spin labelling and distance**  
546 **modelling.** Purified MscL(F88C) was mixed at a 1:1 ratio with deuterated ethylene  
547 glycol and 70  $\mu$ L of the mixture were loaded in a 3 mm quartz tube and flash frozen in  
548 liquid N<sub>2</sub>. PELDOR measurements were performed with a Bruker ELEXSYS E580  
549 pulsed Q band (34 GHz) spectrometer with a TE012 cavity at 50 °K. The offset between  
550 the detection ( $\nu_A$ ) and pump ( $\nu_B$ ) frequencies was 80 MHz and the pulse sequence used  
551 was  $(\pi/2)_A - \tau_1 - \pi_A - (\tau_1+t) - \pi_B - (\tau_2-t) - \pi_A - \tau_2 - \text{echo}^{54}$ .  $\nu_A$  pulses were 16 ns ( $\pi/2$ ) and  
552 32 ns ( $\pi$ ) and separated by  $\tau_1 = 380$  ns, while the  $\nu_B$  pulse was 12 ns long. The shot  
553 repetition time was set to 3 ms. The data acquired were analysed with the DeerAnalysis  
554 2016 Matlab plugin<sup>55</sup>. Time domain spectra were fitted with an exponential decay  
555 function, background-corrected and analysed by Tikhonov regularization<sup>56</sup>. The  
556 validation tool was used as previously described<sup>48</sup>, with the background starting point  
557 varying between 5% and 80% of the length of the trace in 16 steps and 50% random  
558 noise added in 50 trials for each step, resulting in 800 total trials. Finally, datasets more  
559 than 15% above the best (lowest) root-mean-square deviation (RMSD) were discarded.  
560 In silico spin labelling and distance measurements were done using the

561 MTSSLWizard<sup>57</sup> PyMOL plugin, with F88 mutated to C. The “thorough search” option  
562 was used for the MTSSL rotamers and the Van der Waals restraints were set to tight.

563 **Statistical analyses.** Graphs were prepared using SigmaPlot (Systat Software Inc. Ver.  
564 10. Systat Software, Point Richmond, CA, USA). Data in all assays correspond to the  
565 mean values of one to three independent experiments, each one performed in a least  
566 three replicates as mentioned in the corresponding figure legends.

567

568

569

570

571

572

573

574

575

576

577

## 578 **Supporting information**

579 The Supporting Information is available free of charge on the ACS Publications  
580 website. Figure S1, BR2 purification from *E. coli* SuptoxD cultures; Figure S2, MscL  
581 purification from *E. coli* SuptoxR cultures.

## 582 **Abbreviations**

583 MP: membrane protein; DjlA: DnaJ-like protein A; RraA: regulator of ribonuclease  
584 activity A; aTc: anhydrotetracycline; GPCR: G-protein-coupled receptor; BR2:  
585 bradykinin receptor 2; NTR1: neurotensin receptor 1; MscL: large conductance  
586 mechanosensitive ion channel; MscS: small conductance mechanosensitive ion  
587 channel; HtdR, archaeal deltarhodopsin from *Haloterrigena turkmenica*; GFP: green  
588 fluorescent protein; SDS-PAGE: sodium dodecyl sulfate polyacrylamide gel  
589 electrophoresis; WT: Wild type; IMAC: immobilized metal affinity chromatography;  
590 SEC: size-exclusion chromatography; Fos14: fos-choline-14; DDM: n-dodecyl  $\beta$ -D-  
591 maltoside; PELDOR: pulsed electron double resonance; DEER: double  
592 electron double resonance; MTSSL: S-(2,2,5,5-tetramethyl-2,5-dihydro-1H-pyrrol-3-  
593 yl)methyl methanesulfonothioate.

## 594 **Author Contributions**

595 GS conceived and coordinated the project. GS and CP designed the research. MM and  
596 CK carried out the research. MM, CK, CP and GS analyzed the data. GS wrote the  
597 paper with contributions from MM, CK and CP. All authors read and approved the final  
598 manuscript.

599

600 **Competing financial interests**

601 GS is an inventor on a patent application for SuptoxD and SuptoxR  
602 (PCT/EP2017/025168).

603

604 **Acknowledgements**

605 We would like to thank François Baneyx for providing a vector with the gene sequence  
606 of HtdR. This work was supported by a Greek State Scholarships Foundation (Idryma  
607 Kratikon Ypotrofon – IKY) scholarship, funded by the action “Strengthening human  
608 research potential through doctoral research” of the Partnership Agreement  
609 “Development of human potential, education and lifelong learning” 2014-2020, which  
610 is co-financed by the European Structural and Investment Fund (ESIF) and the Greek  
611 State. We also acknowledge support by the project “Synthetic Biology: From omics  
612 technologies to genomic engineering (OMIC-ENGINE)” (MIS 5002636), which is  
613 implemented under the Action “Reinforcement of the Research and Innovation  
614 Infrastructure”, funded by the Operational Programme "Competitiveness,  
615 Entrepreneurship and Innovation" (NSRF 2014-2020) and co-financed by Greece and  
616 the European Union (European Regional Development Fund). CP would like to  
617 acknowledge the Royal Society of Edinburgh, Tenovus (T15/41), Carnegie Trust  
618 (OS000256) grant awards and the School of Biology of the University of St Andrews  
619 for a PhD studentship to CK. PELDOR measurements were performed at the EPR  
620 facilities (Bruker/Q-band E580) and protein identification at the mass spectrometry and  
621 proteomics facility of the University of St Andrews.

622

623 **References**

- 624 1. von Heijne, G. (2007). The membrane protein universe: what's out there and why  
625 bother?. *J. Intern. Med.* 261, 543-557.
- 626 2. Yildirim, M.A., Goh, K.I., Cusick, M.E., Barabasi A.L. & Vidal M. (2007). Drug-  
627 target network. *Nat. Biotechnol.* 25, 1119-1126.
- 628 3. Sarramegna, V., Talmont, F., Demange, P. & Milon, A. (2003). Heterologous  
629 expression of G-protein-coupled receptors: comparison of expression systems from the  
630 standpoint of large-scale production and purification. *Cell. Mol. Life Sci.* 60, 1529-  
631 1546.
- 632 4. Wagner, S., Bader, M.L., Drew, D. & de Gier, J.W. (2006). Rationalizing membrane  
633 protein overexpression. *Trends Biotechnol.* 24, 364-371.
- 634 5. Makino, T., Skretas, G. & Georgiou, G., (2011). Strain engineering for improved  
635 expression of recombinant proteins in bacteria. *Microb. Cell Fact.* 10, 32.
- 636 6. Sarkar, C.A., Dodevski, I., Kenig, M., Dudli, S., Mohr, A., Hermans, E. & Plückthun,  
637 A., (2008). Directed evolution of a G protein-coupled receptor for expression, stability,  
638 and binding selectivity. *Proc. Natl. Acad. Sci. USA* 105, 14808-14813.
- 639 7. Hendrickson, W.A., Horton, J.R. & Lemaster, D.M. (1990). Selenomethionyl  
640 Proteins Produced for Analysis by Multiwavelength Anomalous Diffraction (MAD) -  
641 a Vehicle for Direct Determination of 3-Dimensional Structure. *EMBO J.* 9, 1665-1672.
- 642 8. Gardner, K.H. & Kay, L.E. (1998). The use of <sup>2</sup>H, <sup>13</sup>C, <sup>15</sup>N multidimensional NMR  
643 to study the structure and dynamics of proteins. *Annu. Rev. Bioph. Biom.* 27, 357-406.

- 644 9. Wagner, S., Baars, L., Ytterberg, A.J., Klussmeier, A., Wagner, C.S., Nord, O.,  
645 Nygren, P.A., van Wijk, K.J. & de Gier, J.W. (2007). Consequences of membrane  
646 protein overexpression in *Escherichia coli*. *Mol. Cell. Proteomics*. 6, 1527-1550.
- 647 10. Gubellini, F., Verdon, G., Karpowich, N.K., Luff, J.D., Boel, G., Gauthier, N.,  
648 Handelman, S.K., Ades, S.E. & Hunt J.F. (2011). Physiological response to membrane  
649 protein overexpression in *E. coli*. *Mol. Cell. Proteomics*. 10, M111 007930.
- 650 11. Miroux, B. & Walker, J.E. (1996). Over-production of proteins in *Escherichia coli*:  
651 mutant hosts that allow synthesis of some membrane proteins and globular proteins at  
652 high levels. *J. Mol. Biol.* 260, 289-298.
- 653 12. Gialama, D., Kostelidou, K., Michou, M., Delivoria, D.C., Kolisis, F.N. & Skretas,  
654 G. (2017). Development of *Escherichia coli* Strains That Withstand Membrane Protein-  
655 Induced Toxicity and Achieve High-Level Recombinant Membrane Protein  
656 Production. *ACS Synth. Biol.* 6, 284-300.
- 657 13. Clarke, D.J., Jacq, A. & Holland, I.B. (1996). A novel DnaJ-like protein in  
658 *Escherichia coli* inserts into the cytoplasmic membrane with a type III topology. *Mol.*  
659 *Microbiol.* 20, 1273-1286.
- 660 14. Lee, K., Zhan, X., Gao, J., Qiu, J., Feng, Y., Meganathan, R., Cohen, S.N. &  
661 Georgiou, G. (2003). RraA. a protein inhibitor of RNase E activity that globally  
662 modulates RNA abundance in *E. coli*. *Cell* 114, 623-634.
- 663 15. Gialama, D., Delivoria, D.C., Michou, M., Giannakopoulou, A. & Skretas G.  
664 (2017). Functional Requirements for DjlA- and RraA-Mediated Enhancement of  
665 Recombinant Membrane Protein Production in the Engineered *Escherichia coli* Strains  
666 SuptoxD and SuptoxR. *J. Mol. Biol.* 429, 1800-1816.

- 667 16. Skerra, A. (1994). Use of the tetracycline promoter for the tightly regulated  
668 production of a murine antibody fragment in *Escherichia coli*. *Gene* 151, 131-135.
- 669 17. Drew, D.E., von Heijne, G., Nordlund, P. & de Gier, J.W. (2001). Green fluorescent  
670 protein as an indicator to monitor membrane protein overexpression in *Escherichia coli*.  
671 *FEBS Lett.* 507, 220-224.
- 672 18. Skretas, G. & Georgiou, G. (2009). Genetic analysis of G protein-coupled receptor  
673 expression in *Escherichia coli*: inhibitory role of DnaJ on the membrane integration of  
674 the human central cannabinoid receptor. *Biotechnol. Bioeng.* 102, 357-367.
- 675 19. Skretas, G., Georgiou, G. (2010). Simple genetic selection protocol for isolation of  
676 overexpressed genes that enhance accumulation of membrane-integrated human G  
677 protein-coupled receptors in *Escherichia coli*. *Appl. Environ. Microbiol.* 76, 5852-5859.
- 678 20. Skretas, G., Makino, T., Varadarajan, N., Pogson, M. & Georgiou, G. (2012). Multi-  
679 copy genes that enhance the yield of mammalian G protein-coupled receptors in  
680 *Escherichia coli*. *Metab. Eng.* 14, 591-602.
- 681 21. Wagner, S., Klepsch, M. M., Schlegel, S., Appel, A., Draheim, R., Tarry, M.,  
682 Hogbom, M., van Wijk, K. J., Slotboom, D. J., Persson, J. O., and de Gier, J. W. (2008).  
683 Tuning *Escherichia coli* for membrane protein overexpression. *Proc. Natl. Acad. Sci.*  
684 *USA* 105, 14371-14376.
- 685 22. Schlegel, S., Lofblom, J., Lee, C., Hjelm, A., Klepsch, M., Strous, M., Drew, D.,  
686 Slotboom, D.J. and de Gier, J.W. (2012). Optimizing membrane protein overexpression  
687 in the *Escherichia coli* strain Lemo21(DE3). *J. Mol. Biol.* 423, 648-659.

688 23. Daley, D. O., Rapp, M., Granseth, E., Melen, K., Drew, D., and von Heijne, G.  
689 (2005). Global topology analysis of the Escherichia coli inner membrane proteome,  
690 Science 308, 1321-1323.

691 24. Kim, S. K., Lee, D. H., Kim, O. C., Kim, J. F., and Yoon, S. H. (2017). Tunable  
692 Control of an Escherichia coli Expression System for the Overproduction of Membrane  
693 Proteins by Titrated Expression of a Mutant lac Repressor, ACS Synth. Biol.6, 1766-  
694 1773.

695 25. Angius, F., Ilioaia, O., Amrani, A., Suisse, A., Rosset, L., Legrand, A., Abou-  
696 Hamdan, A., Uzan, M., Zito, F., and Miroux, B. (2018). A novel regulation mechanism  
697 of the T7 RNA polymerase based expression system improves overproduction and  
698 folding of membrane proteins, Sci. Rep. 8, 8572.

699 26. Drew, D., Lerch, M., Kunji, E., Slotboom, D.J. & de Gier, J.W. (2006).  
700 Optimization of amembrane protein overexpression and purification using GFP fusions.  
701 Nat. Methods. 3, 303-313.

702 27. Egloff, P., Hillenbrand, M., Klenk, C., Batyuk, A., Heine, P., Balada, S.,  
703 Schlinkmann, K.M., Scott, D.J., Schütz, M. & Plückthun, A. (2014). Structure of  
704 signaling-competent neurotensin receptor 1 obtained by directed evolution in  
705 Escherichia coli. Proc. Natl. Acad. Sci. USA 111, 655-662.

706 28. Marceau, F. & Regoli, D. (2004). Bradykinin receptor ligands: therapeutic  
707 perspectives. Nat. Rev. Drug Discov. 3, 845-852.

708 29. Kelley, W.L. & Georgopoulos, C. (1997). Positive control of the two-component  
709 RcsC/B signal transduction network by DjlA: a member of the DnaJ family of  
710 molecular chaperones in Escherichia coli. Mol. Microbiol. 25, 913-931.

711

- 712 30. G Geertsma, E.R., Groeneveld, M., Slotboom, D.J. & Poolman, B. (2008). Quality  
713 control of overexpressed membrane proteins. *Proc. Natl. Acad. Sci. USA* 105, 5722-  
714 5727.
- 715 31. Link, A.J., Skretas, G., Strauch, E.M., Chari, N.S. & Georgiou G. (2008). Efficient  
716 production of membrane-integrated and detergent-soluble G protein-coupled receptors  
717 in *Escherichia coli*. *Protein Sci.* 17, 1857-1863.
- 718 32. Kamo, N., Hashiba, T., Kikukawa, T., Araiso, T., Ihara, K. & Nara, T. (2006). A  
719 light-driven proton pump from *Haloterrigena turkmenica*: functional expression in  
720 *Escherichia coli* membrane and coupling with a H<sup>+</sup> co-transporter. *Biochem. Biophys.*  
721 *Res. Com.* 341, 285-290.
- 722 33. Nannenga, B.L. & Baneyx, F. (2011). Enhanced expression of membrane proteins  
723 in *E. coli* with a P(BAD) promoter mutant: synergies with chaperone pathway  
724 engineering strategies. *Microb. Cell Fact.* 10, 105.
- 725 34. Kim, K., Kwon, S.K., Jun, S.H., Cha, J.S., Kim, H., Lee, W., Kim, J., Cho, H.  
726 (2016). Crystal structure and functional characterization of a light-driven chloride  
727 pump having an NTQ motif. *Nat. Commun.* 7, 12677.
- 728 35. Shevchenko, V., Gushchin, I., Polovinkin, V., Round, E., Borshchevskiy, V.,  
729 Utrobin, P., Popov, A., Balandin, T., Büldt, G. & Gordeliy, V. (2014). Crystal structure  
730 of *Escherichia coli*-expressed *Haloarcula marismortui* bacteriorhodopsin I in the  
731 trimeric form. *PLoS One* 9, e112873.
- 732 36. Hochbaum, D.R., Zhao, Y., Farhi, S.L., Klapoetke, N., Werley, C.A., Kapoor, V.,  
733 Zou, P., Kralj, J.M., Maclaurin, D., Smedemark-Margulies, N., Saulnier, J.L., Boulting,  
734 G.L., Straub, C., Cho, Y.K., Melkonian, M., Wong, G.K., Harrison, D.J., Murthy, V.N.,

735 Sabatini, B.L., Boyden, E.S., Campbell, R.E. & Cohen, A.E. (2014). All-optical  
736 electrophysiology in mammalian neurons using engineered microbial rhodopsins. *Nat.*  
737 *Methods* 11, 825-833.

738 37. McIsaac, R.S., Engqvist, M.K., Wannier, T., Rosenthal, A.Z., Herwig, L., Flytzanis,  
739 N.C., Imasheva, E.S., Lanyi, J.K., Balashov, S.P., Gradinaru, V, & Arnold, F.H.  
740 (2014). Directed evolution of a far-red fluorescent rhodopsin. *Proc. Natl. Acad. Sci.*  
741 *USA* 111, 13034-13039.

742 38. C Camponova, P., Baud, S., Matras, H., Duroux-Richard, I., Bonnafous, J.C.,  
743 Marie, J. (2007). High-level expression and purification of the human bradykinin B(2)  
744 receptor in a tetracycline-inducible stable HEK293S cell line. *Protein Expr. Purif.* 55,  
745 300-311.

746 39. Pliotas, C., Ward, R., Branigan, E., Rasmussen, A., Hagelueken, G., Huang, H.,  
747 Black, S.S., Booth, IR., Schiemann, O. & Naismith, J.H. (2012). Conformational state  
748 of the MscS mechanosensitive channel in solution revealed by pulsed electron-electron  
749 double resonance (PELDOR) spectroscopy. *Proc. Natl. Acad. Sci. USA* 109, 2675-  
750 2682.

751 40. Levin, G. & Blount, P. (2004). Cysteine scanning of MscL transmembrane domains  
752 reveals residues critical for mechanosensitive channel gating. *Biophys J.* 86, 2862-  
753 2870.

754 41. Pliotas, C. (2017). Ion Channel Conformation and Oligomerization Assessment by  
755 Site-Directed Spin Labeling and Pulsed-EPR. *Method Enzymol.* 594, 203-242.

756 42. Schiemann, O. & Prisner, T.F. (2007). Long-range distance determinations in  
757 biomacromolecules by EPR spectroscopy. *Q. Rev. Biophys.* 40, 1-53.

758 43. Jeschke, G. (2002). Distance measurements in the nanometer range by pulse EPR.  
759 ChemPhysChem. 3, 927-932.

760 44. Verhalen, B., Dastvan, R., Thangapandian, S., Peskova, Y., Koteiche, H.A.,  
761 Nakamoto, R.K., Tajkhorshid, E., & Mchaourab, H.S. (2017). Energy transduction and  
762 alternating access of the mammalian ABC transporter P-glycoprotein. Nature 543, 738–  
763 741.

764 45. Wingler, L.M., Elgeti, M., Hilger, D., Latorraca, N.R., Lerch, M.T., Staus, D.P.,  
765 Dror, R.O., Kobilka, B.K., Hubbell, W.L. & Lefkowitz, R.J. (2019). Angiotensin  
766 Analogs with Divergent Bias Stabilize Distinct Receptor Conformations. Cell 176, 468-  
767 478

768 46. Bountra, K., Hagelueken, G., Choudhury, H.G., Corradi, V., El Omari, K., Wagner,  
769 A., Mathavan, I., Zirah, S., Wahlgren W., Tieleman, D.P., Schiemann, O., Rebuffat, S.  
770 & Beis, K. (2017). Structural basis for antibacterial peptide self-immunity by the  
771 bacterial ABC transporter McjD. EMBO J. 36, 3062-3079.

772 47. Timachi, M.H., Hutter, C.A., Hohl, M., Assafa, T., Bohm, S., Mittal, A., Seeger,  
773 M.A. & Bordignon, E. (2017). Exploring conformational equilibria of a heterodimeric  
774 ABC transporter. Elife 6, e20236.

775 48. Ackermann, K., Pliotas, C., Valera, S., Naismith, J.H. & Bode, B.E. (2017). Sparse  
776 Labeling PELDOR Spectroscopy on Multimeric Mechanosensitive Membrane  
777 Channels. Biophys. J. 113, 1968-1978.

778 49. Ward, R., Pliotas, C., Branigan, E., Hacker, C., Rasmussen, A., Hagelueken, G.,  
779 Booth, I.R., Miller, S., Lucocq, J., Naismith, J.H. & Schiemann, O. (2014). Probing

780 the structure of the mechanosensitive channel of small conductance in lipid bilayers  
781 with pulsed electron-electron double resonance. *Biophys. J.* 106, 834-842.

782 50. Pliotas, C., Dahl, A.C., Rasmussen, T., Mahendran, K.R., Smith, T.K., Marius, P.,  
783 Gault, J., Banda, T., Rasmussen, A., Miller, S., Robinson, C.V., Bayley, H., Sansom,  
784 M.S., Booth, I.R. & Naismith, J.H. (2015). The role of lipids in mechanosensation. *Nat.*  
785 *Struct. Mol. Biol.* 22, 991-998.

786 51. Chang, G., Spencer, R.H., Lee, A.T., Barclay, M.T. & Rees, D.C. (1998). Structure  
787 of the MscL homolog from *Mycobacterium tuberculosis*: a gated mechanosensitive ion  
788 channel. *Science* 282, 2220-2226.

789 52. Engqvist, M.K., McIsaac, R.S., Dollinger, P., Flytzanis, N.C., Abrams, M., Schor,  
790 S. & Arnold, F.H. (2015). Directed evolution of *Gloeobacter violaceus* rhodopsin  
791 spectral properties. *J. Mol. Biol.* 427, 205-220.

792 53. Branigan, E., Pliotas, C., Hagelueken, G. & Naismith, J.H. (2013). Quantification  
793 of free cysteines in membrane and soluble proteins using a fluorescent dye and thermal  
794 unfolding. *Nat. Protoc.* 8, 2090-2097.

795 54. Martin, R.E., Pannier, M., Diederich, F., Gramlich, V., Hubrich, M. & Spiess, H.W.  
796 (1998). Determination of End-to-End Distances in a Series of TEMPO Diradicals of up  
797 to 2.8 nm Length with a New Four-Pulse Double Electron Electron Resonance  
798 Experiment. *Angew. Chem. Int. Ed. Engl.* 37, 2833-2837.

799 55. Jeschke, G., Chechik, V., Ionita, P., Godt, A., Zimmermann, H., Banham, J.,  
800 Timmel, C.R., Hilger, D. & Jung, H. (2006). DeerAnalysis2006—a comprehensive  
801 software package for analyzing pulsed ELDOR data. *Appl. Magn. Reson.* 30, 473-498.

802 56. Chiang, Y.W., Borbat, P.P. & Freed, J.H. (2005). The determination of pair distance  
803 distributions by pulsed ESR using Tikhonov regularization. *J. Magn. Reson. IM* 172,  
804 279-295.

805 57. Hagelueken, G., Ward, R., Naismith, J.H. & Schiemann, O. (2012). MtsslWizard:  
806 In Silico Spin-Labeling and Generation of Distance Distributions in PyMOL. *Appl.*  
807 *Magn. Reson.* 42, 377-391.

808

809

810

811

812

813

814

815

816

817

818

819

820

821

822

823

824

825

826

827 **Table 1.** Plasmids used in this study.

<b>Plasmid</b>	<b>Protein expressed</b>	<b>Marker</b>	<b>Origin of replication</b>	<b>Source</b>
pASKBR2-EGFP	FLAG-BR2- TEV-EGFP-His <sub>6</sub>	Amp <sup>R</sup>	ColE1	Gialama et al. <sup>12</sup>
pASKNTR1(D03)- EGFP	FLAG- NTR1(D03)- TEV-EGFP-His <sub>6</sub>	Amp <sup>R</sup>	ColE1	Gialama et al. <sup>12</sup>
pASKMscL-EGFP	MscL-EGFP-His <sub>6</sub>	Amp <sup>R</sup>	ColE1	This work
pASKBR2	BR2-His <sub>6</sub>	Amp <sup>R</sup>	ColE1	Link et al.
pASKMscL(F88C)	MscL-His <sub>6</sub>	Amp <sup>R</sup>	ColE1	This work
pASKHtdR	HtdR-His <sub>6</sub>	Amp <sup>R</sup>	ColE1	This work
pSuptoxD	DjlA-His <sub>8</sub>	Cm <sup>R</sup>	ACYC	Gialama et al. <sup>12</sup>
pSuptoxR	RraA-His <sub>8</sub>	Cm <sup>R</sup>	ACYC	Gialama et al. <sup>12</sup>

828

829

830

831

832

833

834

835

836

837 **Table 2.** Membrane proteins studied in this work.

<b>Membrane protein</b>	<b>Organism</b>	<b>Function</b>	<b>Number of TM helices</b>	<b>Topology</b>	<b>Mass (kDa)</b>
BR2	Homo sapiens	Bradykinin receptor 2 (GPCR)	7	N <sup>out</sup> -C <sup>in</sup>	44.5
NTR1(D03)	Rattus norvegicus	Neurotensin receptor 1 variant D03 <sup>6</sup> (GPCR)	7	N <sup>out</sup> -C <sup>in</sup>	44.6
MscL	Mycobacterium tuberculosis	Large conductance mechanosensitive channel	2	N <sup>in</sup> -C <sup>in</sup>	16.0
HtdR	Haloterrigena turkmenica	Deltarhodopsin	7	N <sup>out</sup> -C <sup>in</sup>	27.1

838